Korean J. of Chem. Eng., **13**(4), 343-350 (1996)

A COMPARISON OF CRYSTAL GROWTH KINETICS BY USE OF CHEMICAL POTENTIAL DIFFERENCE AND CONCENTRATION DIFFERENCE

Han Soo Na and Sae Joong Oh*†

Honam Oil Refinery CO., LTD., Yocheon Refinery, Yosu P.O. Box 7, 550-600, Korea
*Dept. of Chemical Engineering, Sun-Moon University, Asan-Kun, Chung Nam 336-840, Korea
(Received 13 July 1995 • accepted 11 April 1996)

Abstract – A Spherical Void Electrodynamic Levitator Trap (SVELT) was used to measure the water activity in the supersaturated aqueous solutions of six materials, NaCl, $(NH_4)_2SO_4$, KH_2PO_4, $NH_4H_2PO_4$, $KAl(SO_4)_2 \cdot 12H_2O$ and glycine. The relationship between chemical potential and concentration was obtained using a fifth order polynomial fit. A comparison of the order of the crystal growth rate obtained from the use of chemical potential difference and concentration difference was made. The order of crystal growth rate calculated from concentration difference was found to be close to that obtained from chemical potential difference at low supersaturation, while at higher supersaturation a deviation was noted.

Key words: *Crystal Growth, Water Activity, Chemical Potential, Supersaturation*

INTRODUCTION

Crystallization is a separation and purification technique to produce a wide variety of materials in chemical and pharmaceutical industries. For crystallizer design, the independent effects of temperature, supersaturation, and solution velocity on the crystal growth rate should be known with reasonable precision.

One of the requirements for crystallization to take place is that the solution must be supersaturated. In a supersaturated solution, solute molecules in the bulk of a solution are transported and integrated into crystal surface, or returned to the solution. Most researchers express the crystallization driving force in terms of the difference in concentration between supersaturated and saturated solution. From the standpoint of thermodynamics, the actual driving force is the chemical potential difference rather than concentration difference. Therefore, how the crystal growth rate relates to the chemical potential difference should be considered.

Crystallization is regarded as a two-stage process, nucleation and growth of nuclei. Nucleation process may be homogeneous or heterogeneous. In heterogeneous nucleation, the formation of crystal nuclei often takes place on the interface between solution and foreign surface. Most commonly, the wall of container or minute particles in solution can serve as catalysts in heterogeneous nucleation when solution concentration exceeds saturation concentration. It is hard to eliminate the effect of solid contact with vessel wall and contaminations in even the most carefully operated conventional experiment. Thus, there are little data available on homogeneous nucleation from solution at high concentration.

In the past few years, the electrodynamic levitator has been used to investigate the thermodynamic and transport properties of aqueous solution at high concentration. In this technique, a single pre-filtered charged solution particle is trapped by the electric field created by the electrodes of the apparatus, and weighed continuously. As it is free of foreign surface, the suspended solution particles can reach very high supersaturation before crystallization occurs.

Arnold [1978] has developed an absolute method for single aerosol particle mass and charge measurement without requiring knowledge of particle shape, density or any adjustable parameter. Tang [1984, 1986] measured the thermodynamic properties of highly supersaturated electrolyte solutions by levitating single micron-sized particles in a controlled water vapor environment. Na [1994] has used a SVELT to investigate homogeneous cluster formation and nucleation in highly supersaturated droplets of NaCl and glycine. The concentration dependent behaviors of the solute activity, the critical size required for nucleation, the interfacial energy of solid to solution, and the diffusion coefficient were estimated nearly up to the spinodal for both systems.

In this work, SVELT was used to measure the water activity of several supersaturated aqueous solutions, and the solute activity was calculated from Gibbs-Duhem equation. Then, the order of crystal growth was determined based on the chemical potential difference of the solute. The order of crystal growth rate was compared with that based on the concentration difference.

CRYSTAL GROWTH KINETICS IN SOLUTION

The diffusion theory of crystal growth is among the oldest theories in this field. The mathematics involved is relatively simple and satisfactory for use in industrial practice [Mullin, 1993; Nyvlt, 1985].

During crystallization, a phase change occurs, connected with mass transfer from the mother phase, that may be a gas, solution or melt. In crystal growth from a supersaturated solution, the dissolved substance must be transported from the bulk

†To whom all correspondences should be addressed.

solution to the crystal surface, where it is incorporated into the crystal lattice. This transport occurs through a stationary solution layer that is in dynamic equilibrium with the crystal surface and with the bulk phase of the supersaturated solution. The crystallization process can be separated into the following steps: transfer of substance to the diffusion layer; diffusion of the substance through the diffusion layer; incorporation of the particles of the substance into crystal lattice; removal of heat released during crystal growth from the crystal into the mother phase.

From the point of view of the crystal growth kinetics, the overall growth rate is determined by the slowest of these processes. Mostly the overall rate-determining step is either diffusion of the substance through the diffusion layer or the incorporation of the species into the crystal lattice. These processes are governed by the difference between concentration at the solid surface and in the bulk of the solution. Starting from Fick's first law, an equation for crystallization was proposed in the form

$$\frac{dm}{dt} = k_m A(C - C^*) \tag{1}$$

On the assumption that there would be a thin stagnant film of liquid adjacent to the growing crystal surface through which molecules of the solute would have to diffuse, Eq. (1) can be modified to the form

$$\frac{dm}{dt} = \frac{D}{\delta} A(C - C^*) \tag{2}$$

Obviously, the thickness of the diffusion layer depends on the relative solid-liquid velocity.

The rate of incorporation of molecules into the crystal lattice depends on the difference in concentrations between the diffusion layer and the crystal surface. Considering an overall concentration driving force, a general equation for crystallization can be written as;

$$\frac{dm}{dt} = kA(C - C^*)^{\alpha} \tag{3}$$

α is an exponent with a value dependent on the conditions, primarily on the supersaturation, and usually referred to as the order of the overall crystal growth process. Thus, the growth rate equation may be written as

$$R_g = \frac{1}{A}\frac{dm}{dt} = k(C - C^*)^{\alpha} \tag{4}$$

Both the exponent and crystal growth coefficient can be determined by the measurement of crystal growth rates under different conditions. This equation can be written in terms of relative supersaturation.

$$R_g = k\Delta C^{\alpha} = K\left(\frac{C}{C^*} - 1\right)^{\alpha} = K\sigma^{\alpha} \tag{5}$$

From the viewpoint of thermodynamics, the driving force of crystallization is expressed as

$$\Delta\mu = \mu - \mu^* \tag{6}$$

The chemical potential difference is related to the activity ratio of solute as Eq. (7).

$$\mu - \mu^* = \nu RT \ln\left(\frac{a}{a^*}\right) \tag{7}$$

The thermodynamic relative supersaturation is defined as

$$\sigma_a = \frac{a - a^*}{a^*} \tag{8}$$

Based on the assumption of $\ln(1+\sigma_a)=\sigma_a$ in the whole supersaturation region, the crystal growth rate equation is then expressed thermodynamically as

$$R_g = k'\Delta\mu^{\alpha'} = K'\left(\frac{\Delta\mu}{\nu RT}\right)^{\alpha'} = K'\sigma_a{}^{\alpha'} \tag{9}$$

The ratio of the thermodynamic driving force to concentration driving force of crystallization is then

$$\frac{\sigma_a}{\sigma} = \frac{\gamma_{\pm}}{\gamma_{\pm}^*} + \frac{\frac{\gamma_{\pm}}{\gamma_{\pm}^*} - 1}{\frac{C}{C^*} - 1} \tag{10}$$

From Eq. (10), $\gamma_{\pm}/\gamma_{\pm}^* = 1$ is valid through whole concentration range for an ideal solution. For non-ideal solutions, the more the equation $\gamma_{+}/\gamma_{+}^* = 1$ differs from unity, the greater difference there is between the thermodynamic driving force and concentration driving force of crystallization.

In principle, the measurement methods of crystal growth rate can be divided into two groups, direct and indirect methods. The most commonly used methods are summarized in detail [Nyvlt, 1985]. Mullin [1967] and Li [1992] measured the linear crystal growth rates of ammonium dihydrogen phosphate, potassium dihydrogen phosphate, and glycine by using direct measurement methods. The crystal growth rates of aluminum potassium sulfate and sodium chloride (NaCl) in a fluidized bed crystallizer had been measured by Garside and Mullin [1968], and Rumford and Bain [1960]. Mullin [1970] had measured ammonium sulfate by using an indirect measurement method.

The choice of method depends on further treatment of measured data. The crystal growth is affected by many factors and that each measurement method has its own advantages and disadvantages. Thus, the experimental conditions and data requirements for each given system should be examined carefully to determine the experimental method.

EXPERIMENTAL

1. Materials

In this work, NaCl, $(NH_4)_2SO_4$, ammonium dihydrogen phosphate (ADP), potassium dihydrogen phosphate (KDP), KAl $(SO_4)_2 \cdot 12H_2O$ (K-alum) and glycine were used as solutes. All of these chemicals have purities higher than 99.9%, and were purchased from Aldrich Chemical Co.

2. Procedures

The principal parts of the apparatus to be used in the ex-

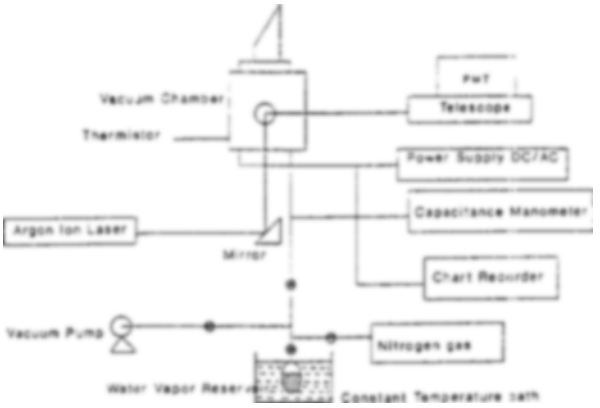

Fig. 1. Schematic of experimental apparatus

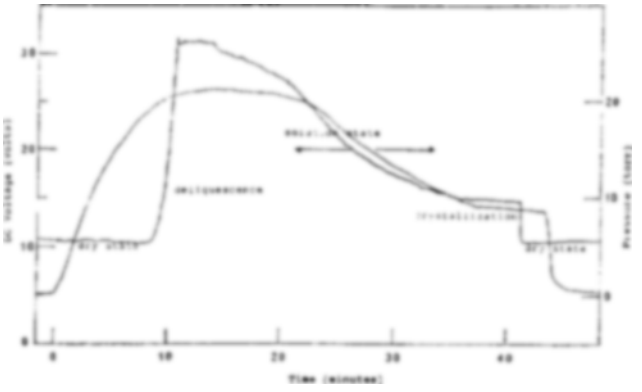

Fig. 2. Variation of DC voltage and vapor pressure versus time recorded by chart recorder during a typical experiment for $(NH_4)_2SO_4$.

periments are the electrodynamic levitator encased in a vacuum chamber, a particle generator, the vacuum system, and the optics. The configuration of experimental apparatus is shown schematically in Fig. 1.

Laboratory measurements are performed with charged salt particle suspended in SVELT [Arnold and Folan, 1987; Arnold, 1991] placed in vacuum chamber equipped with a water reservoir that can maintain the temperature at 25 ± 0.1°C.

Solution particles can be charged by adding a ring electrode in front of the nozzle of the particle generator. Charged particles may be trapped in the SVELT with a moderate AC voltage. Introducing a DC potential allows the particle to be brought to the trap center.

For a stationary particle at the null point, the weight, mg, of the particle carrying q electrostatic charges is balanced against electrical force;

$$mg = Cq\frac{V_{dc}}{Z_o} \tag{11}$$

The value of C is not required for relative measurement and is only needed to determine the absolute mass of the suspended particle. As a result of water vapor evaporation or condensation, the relative mass change can be measured as precisely as one can measure the DC voltage changes necessary for positioning the particle to the null point. The saturation ratio of pressure in solution droplet is equal to the water activity of the solution, of which relation is shown as

$$a_w = \frac{P_w}{P_w^*} \tag{12}$$

By adjusting the humidity of the chamber, the weight of the suspended particle and thus the desired concentration of the solution can be achieved.

Experimental procedure is also described in detail [Na, 1994]. A solution to be studied was prepared by adding a small quantity of solid to 100 ml of deionized water. The solution was subsequently filtered through a Millipore filter directly into droplet generator to remove dust or solid contaminants which causes heterogeneous nucleation. The charged particles entering the levitator (ejection velocity about 1 m/sec) are easily caught in the trap with a moderate AC voltage. The electric field null point at the center of the chamber was illuminated with the argon ion laser beam. A particle trapped in the centermost region of the chamber was observed through the laser light scattered at 90°C to the incident beam. This allowed one to stabilize the particle in the region of minimum electric field by manual adjusting the voltage controls. The chamber was sealed and evacuated to a pressure below 10^{-5} torr. The DC balancing voltage corresponding to the dry particle mass was recorded to calculate the concentration of the microparticle accurately. After the DC voltage of the dry particle was recorded, water vapor above the vapor reservoir was allowed to bleed back slowly into the chamber. The vapor reservoir allowed the particle to deliquescence when the vapor pressure in the chamber exceeded the vapor pressure of saturated solution of droplet. A second evacuation was then commenced at a slower rate by adjusting the needle valve. This procedure caused the solution droplet to be supersaturated. Thereafter, evacuation was continued at a slower rate until the crystallization point.

After crystallization, the evacuation was continued to insure that there has been no charge loss during the cycle. During the run, DC balancing voltage was continuously tuned in order to retain the particle at the center of the electrodynamic trap and the DC balancing voltage and pressure inside the chamber were recorded.

RESULTS AND DISCUSSIONS

Fig. 2 shows the variation of the DC balancing voltage and absolute pressure typically for an ammonium sulfate particle undergoing the complete cycle of deliquescence, evaporation and crystallization. The balancing DC voltage of dry particle corresponds to the base line. Water vapor is gradually increased at a slower rate. Until deliquescence occurs, no change is found in the DC balancing voltage. The abrupt change in particle mass at the deliquescence point is clearly evident from the DC balancing voltage rise.

Once the particle had taken on water from the vapor environment, the pressure in the chamber stabilizes to the vapor pressure above the water vapor reservoir. As a result of water vapor evaporation, the DC balancing voltage decreases steadily

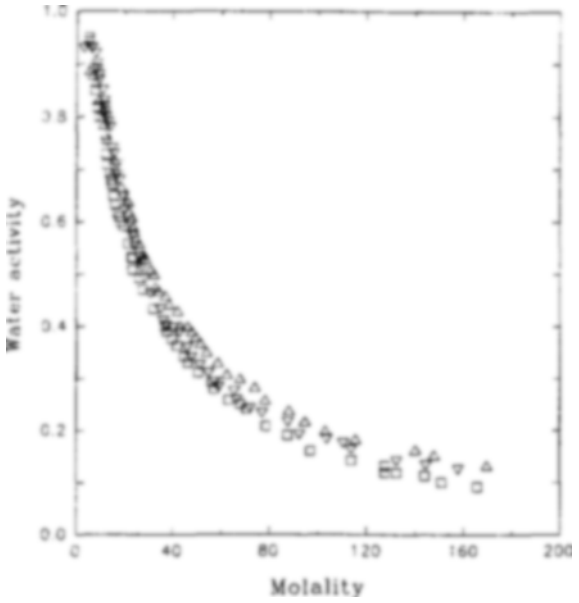

Fig. 3. Water activity vs molality for ADP-water system at 25°C. Each symbol represents the different data-set of which the experiment was repeated at the same conditions in Fig. 3 through 8.

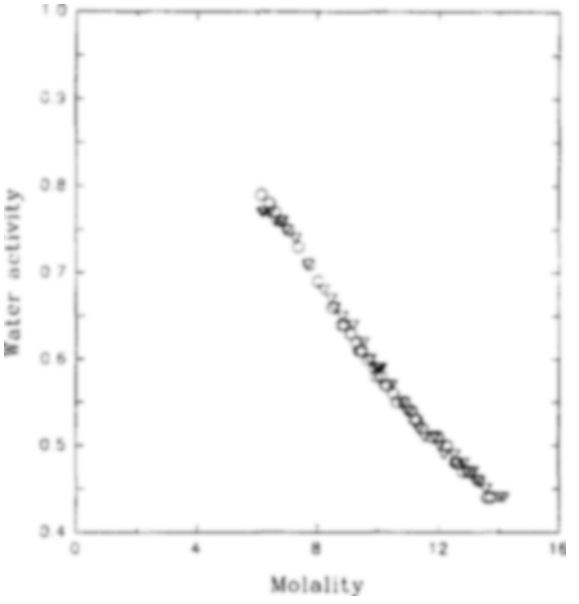

Fig. 4. Water activity vs molality for NaCl-water system at 25°C.

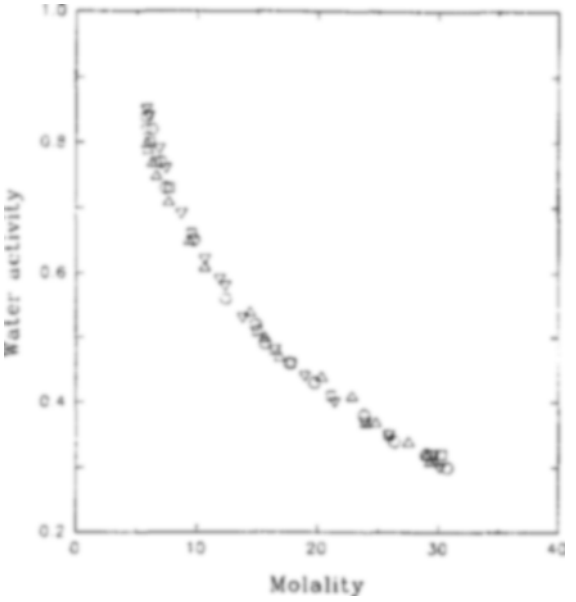

Fig. 5. Water activity vs molality for $(NH_4)_2SO_4$-water system at 25°C.

and solution droplet becomes supersaturated and eventually crystallized. The DC balancing voltage near the end of cycle drops precipitously indicating a phase transition at the crystallization point.

The particle responds rapidly to the ambient vapor pressure and small micron-sized droplet reaches phase equilibrium within a second. Therefore, the entire experiment with absorption, evaporation, crystallization processes could be performed in a few hours. Thus, this experimental technique offers a relatively fast way to obtain water activity data up to higher supersaturation range.

The water activities of various solutions at 25°C are shown in Fig. 3 to 8. The activity were measured over the supersaturated region up to the critical concentration by using the electrodynamic technique. Same experiments were repeated a few times for the same solutions, which were distinguished by different symbols in Fig. 3 to 8. The uncertainties in determining the particle balance voltage of dry particle droplets are at most 0.01 for all systems studied. The corresponding uncertainties in molality of the droplet suspended at crystallization point were approximately 2% to 3%. The experimental data-sets in Fig. 3 to 8 showed very good reproducibility within the experimental uncertainties.

Cohen [1987] also reported water activity data for aqueous electrolyte solutions at 20°C using a bihyperboloidal electrodynamic balance trap in a continuous flowing system. The change in the water activity is generally negligible in the temperature range of 20°C to 30°C. Comparing the water activity data at 20°C from Cohen [1987] with ours at 25°C, the differences were at most 0.02 (±3%) in the worst case for NaCl-H_2O and $(NH_4)_2SO_4$-H_2O systems.

Tang and Munkelwitz [1984] observed crystal nucleation concentration at 25°C for the NaCl-H_2O and the $(NH_4)_2SO_4$-H_2O systems using the electrodynamic balance technique in a continuous flowing system. They reported crystallization concentrations to be 11.2 and 29.9 M (molality), respectively for both systems.

Richardson and Spann [1984] also have measured crystallization concentration of $(NH_4)_2SO_4$ aqueous solution, of which system is similar to that used in our study. They found that the concentration of the solution at crystallization was 36.05 M± 0.4 at 24°C.

It should be pointed out that through the electrodynamic balance technique used in the present work we achieved extremely high supersaturation. It is clear that the maximum attainable supersaturations obtained by the conventional bulk

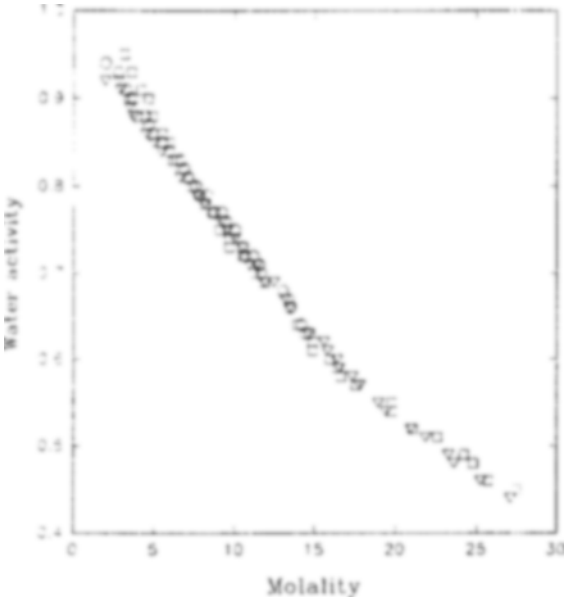

Fig. 6. Water activity vs molality for KDP-water system at 25°C.

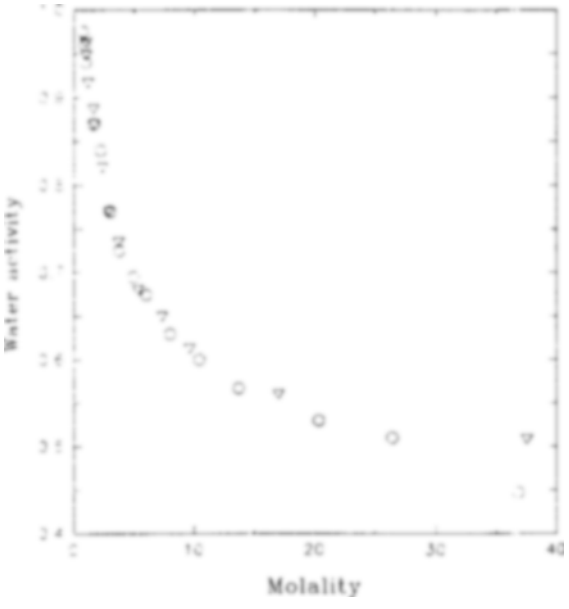

Fig. 7. Water activity vs molality for aluminum potassium sulfate-water system at 25°C.

cooling methods to determine the border of the metastable are much lower. This is due to the solute crystallization induced by heterogeneous nucleation on container surface or on minute particles in solution.

The metastable state is a quasi-stable state in which the solution appears to be in equilibrium, but as time passes the solution properties change. In our experiments, however, we did not observe any time dependent effect on crystallization concentrations and water activities. This is likely due to the long time scale required to observe these effects.

The solute activity of solutions can be evaluated at various concentrations, using the Gibbs-Duhem equation, with the water activity data shown in Fig. 3 through 8. Then, the chemical

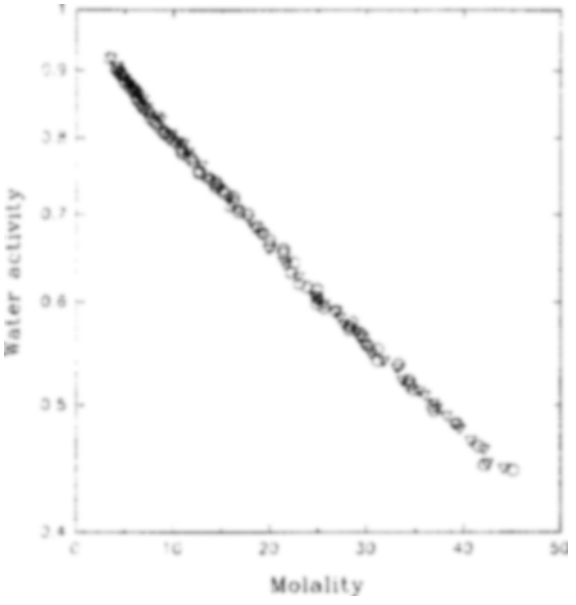

Fig. 8. Water activity vs molality for glycine-water system at 25°C.

Table 1. Physical properties of studied substances

Substance	m.w	m*	d	ν
ADP	115.03	3.48	1.80	2
NaCl	58.48	6.11	2.17	2
$(NH_4)_2SO_4$	132.14	5.80	1.77	3
KDP	136.09	1.63	2.34	2
K-alum	474.39	0.29	1.72	3
Glycine	75.07	3.34	1.16	1

m.w.: molecular weight (g/mol)
m*: solubility at 25°C (molality)
d: density (g/cm^3)
ν: ionic number

potential difference is determined using Eq. (7). ν is equal to unity for nonelectrolyte in Eq. (7). In this work, a fifth order polynomial was chosen to express the relationship between the solute activity ratio and the concentration. The coefficients of polynomial of each system studied are listed in Table 2. The concentration range for which the polynomial fit is valid lies between the saturation point and the crystallization point, that is, the concentration range covers the whole metastable region.

In Table 3, chemical potential and concentration difference at specified relative supersaturation are listed for each system studied.

The crystal growth rate data were extracted from the literatures [Garside and Mullin, 1968; Li, 1992; Mullin and Amatavivadhana, 1967; Mullin, 1970; Rumford and Bain, 1960]. All data units were converted for consistency. The units used are molality for concentration and $kg/m^2/sec$ for crystal growth rate. The growth rate data can be then plotted versus concentration difference using a logarithmic plot. Taking logarithms on both sides of Eq. (5), it becomes

$$\log R_g = \alpha \log \Delta C + \log k \tag{13}$$

Table 2. Coefficients of fitted functions for ln(a/a*) versus m

$\ln(a/a^*)=C_0+C_1m+C_2m^2+C_3m^3+C_4m^4+C_5m^5$

Substance	C_0	C_1	C_2	C_3	C_4	C_5
ADP	1.4175	6.4945E-1	-9.0854E-2	6.9729E-3	-2.5997E-4	3.7082E-6
NaCl	7.6460E-1	-5.9440E-1	9.0280E-2	-7.4840E-3	3.5050E-4	1.2828E-5
$(NH_4)_2SO_4$	1.0856	2.9440E-1	-2.1350E-2	1.0230E-3	-2.7086E-5	2.8990E-7
KDP	-7.0589E-1	5.2071E-1	-5.4631E-2	3.3781E-3	-1.0465E-4	1.2496E-6
K-alum	-7.7093E-1	2.6990	1.7340E-1	-8.5905E-1	3.3545E-1	-4.0032E-2
Glycine	1.2891	5.2670E-1	-3.7650E-2	1.4670E-3	-2.8030E-5	2.0604E-7

Table 3. Concentration and chemical potential difference for specified supersaturations

	ADP		NaCl		$(NH_4)_2SO_4$	
σ	ΔC	Δμ	ΔC	Δμ	ΔC	Δμ
0.01	0.0348	0.0079	0.0611	0.0120	0.0580	0.0075
0.05	0.1740	0.0389	0.3055	0.0619	0.2900	0.0371
0.10	0.3480	0.0757	0.6110	0.1281	0.5800	0.0729
0.15	0.5220	0.1106	0.9165	0.1978	0.8700	0.1074
0.20	0.6960	0.1437	1.2220	0.2705	1.1600	0.1407
0.25	0.8700	0.1751	1.5275	0.3452	1.4500	0.1729
0.30	1.0440	0.2050	1.8330	0.4213	1.7400	0.2039

	KDP		K-alum		Glycine	
σ	ΔC	Δμ	ΔC	Δμ	ΔC	Δμ
0.01	0.0163	0.0060	0.0029	0.0076	0.0334	0.0107
0.05	0.0815	0.0297	0.0145	0.0378	0.1670	0.0528
0.10	0.1630	0.0589	0.0290	0.0754	0.3340	0.1042
0.15	0.2445	0.0876	0.0435	0.1129	0.5010	0.1544
0.20	0.3260	0.1158	0.0580	0.1501	0.6680	0.2032
0.25	0.4075	0.1435	0.0725	0.1872	0.8350	0.2508
0.30	0.4890	0.1707	0.0870	0.2240	1.0020	0.2971

σ: relative supersaturation

ΔC: concentration difference (molality)

Δμ: chemical potential difference (J/mol)

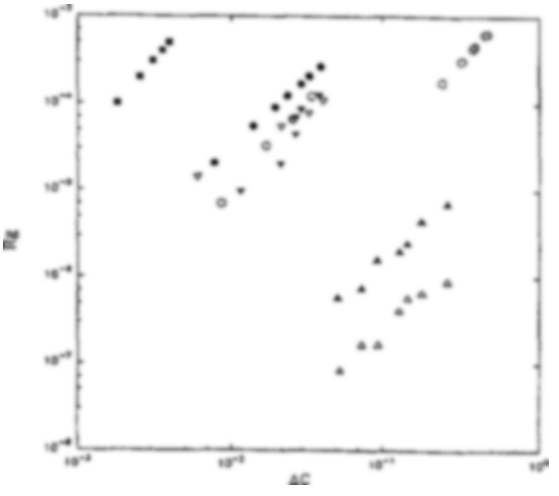

Fig. 9. Growth rate vs concentration difference.

○: NaCl, ●: K-alum, ○: KDP, ■: ADP, △: (010) of glycine, ▲: (011) of glycine, ▽: (100) of $(NH_4)_2SO_4$, ▼: (011) of $(NH_4)_2SO_4$

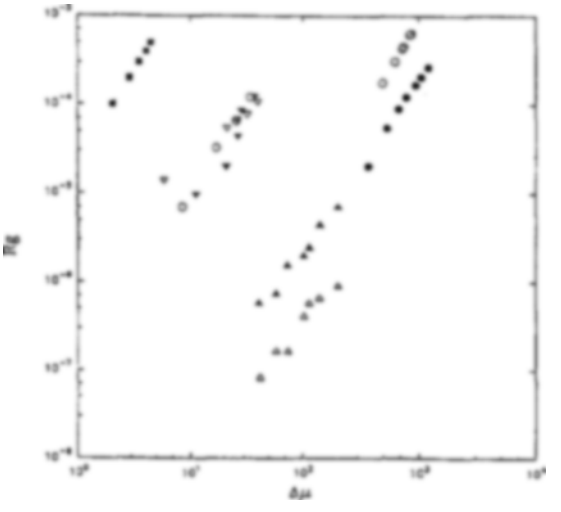

Fig. 10. Growth rate vs chemical potential difference.

○: NaCl, ●: K-alum, ○: KDP, ■: ADP, △: (010) of glycine, ▲: (011) of glycine, ▽: (100) of $(NH_4)_2SO_4$, ▼: (011) of $(NH_4)_2SO_4$

It is obvious that the relationship between crystal growth rate and concentration difference should be represented as a straight line on a logarithmic plot. Those results are shown in Fig. 9 for all systems.

From the standpoint of thermodynamics, the driving force for crystallization in the crystal growth rate equation should be chemical potential instead of concentration. Eq. (9) represents the crystal growth rate in terms of chemical potential. Eq. (9) can be rewritten as

$$\log R_g = \alpha' \log \Delta\mu + \log K' \tag{14}$$

The growth rate data were recalculated and plotted against chemical potential difference. The results are shown in Fig. 10. The crystal growth rate also increases linearly in the logarithmic plot. The order of crystal growth in Eq. (13) and (14) are summarized in Table 4. The order of crystal growth rate calculated from concentration difference was consistent with that calculated from chemical potential difference when the measurements of crystal growth rate were performed in the lower supersaturation region. However, large deviations between the order calculated from chemical potential and that obtained from concentration were found for KDP and K-alm. The deviation is considered to be non-ideal behavior resulting from relatively high supersaturation.

Consequently, the order of crystal growth rate should be calculated by using the chemical potential difference as the driv-

Table 4. Order of crystal growth rate equation and relative supersaturation range in growth rate measurements

Substance		α	α'	α^T	σ range
ADP		2.0	2.0	2.0[1]	0.0005-0.0017
NaCl		2.0	2.0	2.0[1]	0.0014-0.0057
$(NH_4)_2SO_4$	(100)	1.0	1.0	1.0[2]	0.0010-0.0071
	(001)	2.2	2.2	2.0[2]	0.0020-0.0067
KDP		2.0	2.3	2.0[1]	0.1482-0.2848
K-alum		1.6	2.2	1.6[3]	0.0263-0.1352
Glycine	(010)	1.6	1.6	1.3[4]	0.0159-0.0777
	(011)	1.6	1.6	1.5[4]	0.0154-0.0779

α: order of growth rate equation calculated from concentration difference
α': order of growth rate equation calculated from chemical potential difference
α^T: order of growth rate equation obtained from literature
σ range: range of relative supersaturation during growth rate measurements
[1]: extracted from Nyvlt [1985]
[2]: extracted from Mullin [1970]
[3]: extracted from Garside [1968]
[4]: extracted from Li [1992]

ing force of crystallization at higher supersaturation. The crystal growth rate equation expressed in terms of concentration must be a close approximation only in relatively low supersaturation region.

CONCLUSIONS

Traditionally, concentration difference was used in the crystal growth rate equation as the driving force of crystallization. In actual situation, in order to lead to an exact expression, the thermodynamic definition must be used. The driving force of crystallization is expressed thermodynamically as the chemical potential difference of the crystalline substance between supersaturated solution and saturated solution.

The electrodynamic balance technique in which a single micron-sized solution droplet is levitated has been shown to be useful for investigating thermodynamic properties of supersaturated solution. The measurement of the water activities were made far into the metastable zone and approached the spinodal curve.

The data measured are used, in conjunction with solution thermodynamics and crystal growth theory, to examine the order of crystal growth rate in the high supersaturated region.

NOMENCLATURE

A : crystal surface area [m^2]
C : geometric constant, concentration [molality]
D : diffusion constant [m^2/sec]
K : proportional constant [$Kg/m^2/sec$]
P : vapor pressure of water [mmHg]
R : gas constant [J/Kmol/°K]
R_g : crystal growth rate [$Kg/m^2/sec$]
T : absolute temperature [°K]
V_{dc} : dc voltage [volts]
Z_o : characteristic length of cell [cm]
a : solute activity, dimensionless
a_w : water activity, dimensionless
d : density [g/cm^3]
g : gravitational constant [cm/sec^2]
k : proportional constant [$Kg/m^2/sec/(\Delta C)^\alpha$]
k_m : coefficient of mass transfer [$Kg/m^2/sec/(\Delta C)$]
m : mass of solid [g]
q : charge of particle [coulomb]
t : time [sec]

Greek Letters

α : order of crystal growth rate equation, dimensionless
γ : mean solute activity coefficient, dimensionless
Δ : difference, dimensionless
δ : diffusion layer thickness [m]
μ : chemical potential [J/mol]
ν : ionic number, dimensionless
σ : relative supersaturation, dimensionless
σ_a : thermodynamic relative supersaturation, dimensionless

Superscripts

* : saturation state
' : parameters used in thermodynamic expression of crystal growth rate equation

Subscripts

w : water
+ : cation
− : anion

REFERENCES

Arnold, S., "A Three-axis Spherical Void Electrodynamic Levitator Trap for Microparticle Experiments", *Rev. Sci. Instru.*, **62**(12), 3025 (1991).
Arnold, S., "Determination of Particle Mass and Charge by One Electron Differentials", *J. Aerosol. Sci.*, **10**, 49 (1978).
Arnold, S. and Folan, L. M., "Spherical Void Electrodynamic Levitator", *Rev. Sci. Instru.*, **58**(9), 1732 (1987).
Cohen, M. D., Flagen, R. C. and Seinfeld, J. H., *J. Phys. Chem.*, **91**, 4563 (1987).
Garside, J. and Mullin, J. W., "The Crystallization of Aluminum Potassium Sulfate: A Study in the Assessment of Crystallizer Design Data. Part III. Growth and Dissolution Rates", *Trans. Inst. Chem. Engrs.*, **46**, T11 (1968).
Larsen, M. A. and Mullin, J. W., "Crystallization Kinetics of Ammonium Sulfate", *J. Cryst. Growth*, **20**, 183 (1973).
Li, L. and Rodriguez-Hornedo, N., "Growth Kinetics and Mechanism of Glycine Crystals", *J. Cryst. Growth*, **121**, 33 (1992).
Mullin, J. W., "Crystallization", 3rd ed., Butterworth (1993).
Mullin, J. W. and Amatavivadhana, A., "Growth Kinetics of Ammonium and Potassium-dihydrogen Phosphate Crystals", *J. Appl. Chem.*, **17**, 151 (1967).
Mullin, J. W., Chakraborty, M. and Mehta, K., "Nucleation and Growth of Ammonium Sulfate Crystals from Aqueous Solution", *J. Appl. Chem.*, **20**, 367 (1970).

Myerson, A. S., "Handbook of Industrial Crystallization", Butterworth (1993).

Na, H.-S., Arnold, S. and Myerson, A. S., "Cluster Formation in Highly Supersaturated Solution Droplets", *J. Cryst. Growth*, **139**, 104 (1994).

Nicolau, I. F., "Growth Kinetics of Potassium-Dihydrogen Phosphate Crystals in Solution", *Krist. Tech.*, **9**(11), 1255 (1974).

Nyvlt, J., Sohnel, O., Matuchova, M. and Broul, M., "The Kinetics of Industrial Crystallization", Elsevier (1985).

Prausnitz, J. M., Lichtenthaler, R. N. and Azevedo, E. G., "Molecular Thermodynamics of Fluid-Phase Equilibria", 2nd ed., Prentice-Hall (1986).

Richardson, C. B. and Spann, J. F., *J. Aerosol Sci.*, **15**, 563 (1984).

Robinson, R. A. and Stokes, R. H., "Electrolyte Solution", 2nd ed., Butterworth (1959).

Rumford, F. and Bain, "The Controlled Crystallization of Sodium Chloride", *J. Trans. Inst. Chem. Engrs.*, **38**, 10 (1960).

Tang, I. N. and Munkelwitz, H. R., "An Investigation Solute Nucleation in Levitated Solution Droplets", *J. Colloid and Interface Sci.*, **98**(2), 430 (1984).

Tang, I. N., Munkelwitz, H. R. and Wang, N., "Water Activity Measurements with Single Suspended Droplets: The NaCl-H_2O and KCl-H_2O Systems", *J. Colloid and Interface Sci.*, **114**(2), 409 (1986).